Review

Platelet Biorheology and Mechanobiology in Thrombosis: In Silico Perspectives

Rukiye Tuna , Wenjuan Yi , Esmeralda Crespo Cruz , JP Romero , Yi Ren , Jingjiao Guan , Yan Li , Yuefan Deng , Danny Bluestein , Z. Leonardo Liu * , Jawaad Sheriff *

Posted Date: 14 February 2024

doi: 10.20944/preprints202402.0799.v1

Keywords: von Willebrand factor; platelet margination; platelet adhesion; shear-induced platelet aggregation; platelet mechanobiology; biorheology; platelet activation; thrombosis

Review

Platelet Biorheology and Mechanobiology in Thrombosis: *In Silico* Perspectives

Rukiye Tuna [1], Wenjuan Yi [1], Esmeralda Crespo Cruz [1], JP Romero [1], Yi Ren [2], Jingjiao Guan [1,3], Yan Li [1,3], Yuefan Deng [4], Danny Bluestein [5], Z. Leonardo Liu [1,3,*] and Jawaad Sheriff [5,*]

[1] Department of Chemical & Biomedical Engineering, FAMU-FSU College of Engineering, Tallahassee, FL, USA
[2] Department of Biomedical Sciences, College of Medicine, Florida State University, Tallahassee, FL, USA
[3] Institute for Successful Longevity, Florida State University, Tallahassee, FL, USA
[4] Department of Applied Mathematics and Statistics, Stony Brook University, Stony Brook, NY, USA
[5] Department of Biomedical Engineering, Stony Brook University, Stony Brook, NY, USA
* Correspondence: jawaad.sheriff@stonybrook.edu, leo.liu@eng.famu.fsu.edu

Abstract: Thrombosis is the pathological clot formation under abnormal hemodynamic conditions, which can result in vascular obstruction, causing ischemic strokes and myocardial infarction. Thrombus growth under moderate to low shear (<1000 s^{-1}) relies on platelet activation and coagulation. Thrombosis at elevated high shear rates (>10,000 s^{-1}) is predominantly driven by unactivated platelet binding and aggregating mediated by von Willebrand factor (VWF), while platelet activation and coagulation are secondary in supporting and reinforcing the thrombus. Given the molecular and cellular level information it can access, multiscale computational modelling informed by biology can provide new pathological mechanisms that are otherwise not accessible experimentally, holding promise for novel first-principle-based therapeutics. In this review, we summarize the key aspects of platelet mechanobiology, focusing on the molecular and cellular scale events and how they build up all the way to thrombosis through platelet adhesion and aggregation in the presence or absence of platelet activation. In particular, we highlight the recent advancements in multiscale modelling of platelet biorheology and mechanobiology and their role in predicting thrombus formation. Recent applications of artificial intelligence in modelling platelet mechanobiology and thrombosis have also been briefly discussed.

Keywords: von Willebrand factor; platelet margination; platelet adhesion; shear-induced platelet aggregation; platelet mechanobiology; biorheology; platelet activation; thrombosis.

1. Introduction

Thrombosis in vascular disease is triggered by the interaction of blood constituents with an injured blood vessel wall and non-physiologic flow patterns characteristic of cardiovascular pathologies. The process for arterial thrombus formation in a high-shear environment differs from that for low-shear thrombosis (such as deep venous thrombosis), mostly governed by the Virchow Triad, which postulates that thrombosis is governed by three components: endothelial wall damage, stasis of blood flow, and hypercoagulability [1]. Thrombus formation at a high shear rate is mediated by an alternative triad, a combination of von Willebrand factor (VWF), a high shear environment, and a thrombotic surface (e.g., subendothelial collagen matrix) [2–5]. Recent studies have shown that VWF plays a vital role in high-shear thrombus formation [3,4,6] through a process called shear-induced platelet aggregation (SIPA), which entails the rapid binding and entanglement of VWF polymers with inactivated platelets under elevated high shear rates (>10,000 s^{-1}) [7]. The SIPA process involves three sequential stages [3]:(1) VWF elongation, (2) platelet aggregation, and (3) agglomerate capture. Stage 1 involves the conformational change of VWF from globular to elongated state that reveals many A1 domains to bind platelet glycoprotein Ibα (GPIbα) receptors in the flow. Stage 2 is associated with forming platelet agglomerates resulting from GPIbα-VWF A1 binding. In this stage, GPIbα-VWF A1 interactions lead to

 doi:10.20944/preprints202402.0799.v1

high-shear platelet tethering and Mechanotransduction- and biochemical mediator-facilitated platelet activation [8–11]. In Stage 3, the platelet agglomerate approaches the immobilized VWF surface, rolls, and translates on the surface until fully captured before platelet activation that further reinforces the accumulation of platelets via $\alpha_{IIb}\beta_3$-fibrinogen binding.

The disparate spatio-temporal scales between molecular-level inter- and intra-platelet events to macroscopic transport in blood flow pose a major modelling and computational challenge, which requires careful selection of models of specific scales or even integration of multiple numerical techniques suitable for distinct scales. Molecular dynamics (MD) allows for atomistic interactions (i.e., GP1b-A1 binding [12], integrin $\alpha_{IIb}\beta_3$-fibrinogen binding [13], etc.) with high fidelity. However, MD is computationally cost-prohibitive and is limited to nanometer length-scales events that occur mostly within nanoseconds or microseconds. Lattice-Boltzmann method and Dissipative Particle Dynamics (DPD) as mesoscopic methods can be used to model blood as a polydisperse particulate fluid, promising to address micro- to millisecond scale events that often flow-mediated binding occurs, which are critical for macroscopic growth or embolization [14–17]. Continuum approaches represent platelet accumulation or coagulation by field equations and moving boundaries, which permits shape change with interfaces of different properties and time scales [18,19]. Continuum systems, however, are limited to macroscopic fluid scales that homogenize the microscale details and require careful closure of the system of equations through constitutive relations [20,21].

The following sections describe the various approaches to modelling platelet mechanobiology, its role in thrombus formation, and the innovative multiscale approaches used to elucidate the complex nature of thrombosis. These sections are divided by the major (not necessarily sequential) steps in thrombus formation: platelet margination, adhesion, activation, and aggregation. This is followed by a brief description of recent works on using artificial intelligence (AI) to enhance multiscale modelling of platelet mechanobiology.

2. Platelet Margination

Platelet margination is a physiological phenomenon that occurs as platelets migrate toward the vessel wall and get retained in the cell-free layer (CFL), where red blood cells (RBCs) are hydrodynamically depleted [22,23]. Margination could enhance the near-wall platelet concentration [24] and has been found to support the attachment of platelets and subsequent platelet clot formation [25] (Figure 1a). Over the past decade, computational particulate flow techniques have emerged to quantify the rheological nature of margination at cellular scales.

Crowl and Fogelson [23] examined how platelet margination varies with shear rate, hematocrit, and platelet size through a two-dimensional (2D) lattice Boltzmann-immersed boundary method. Using a three-dimensional (3D) boundary integral method, Zhao and Shaqfeh [26], Zhao et al. [27] showed that particle margination correlates with the fluctuations of velocity fields me-diated by RBC interactions in the suspension to understand the platelet margination mechanism at vessel walls (Figure 1b). Combining theory and computation, Kumar and Graham [28,29] attributed the margination and segregation of cells to the heterogeneous pair collision due to disparities in cell rigidity. Using a 3D lattice Boltzmann-based method, Reasor et al. [25] found that the margination rate increases with hematocrit and spherical particles marginate faster than disk-shaped platelets. Combining 3D simulations and scaling analysis, Mehrabadi et al. [22] showed that the margination length scales cubically with vessel sizes and is independent of shear rate. They estimated that it would take $\sim$ 20 mm for platelets to fully marginate within a 40 μm diameter vessel. Using a multiscale particulate blood flow solver, Liu et al. [30,31] demonstrated that particles need to be at least 1 μm in size to give rise to margination (Figure 1c). Furthermore, the same group quantified the full diffusion rate tensor of platelets trans-ported in blood flows, providing a more accurate constitutive relation for continuum-level computational modelling of platelet transport in blood flows [32].

 doi:10.20944/preprints202402.0799.v1

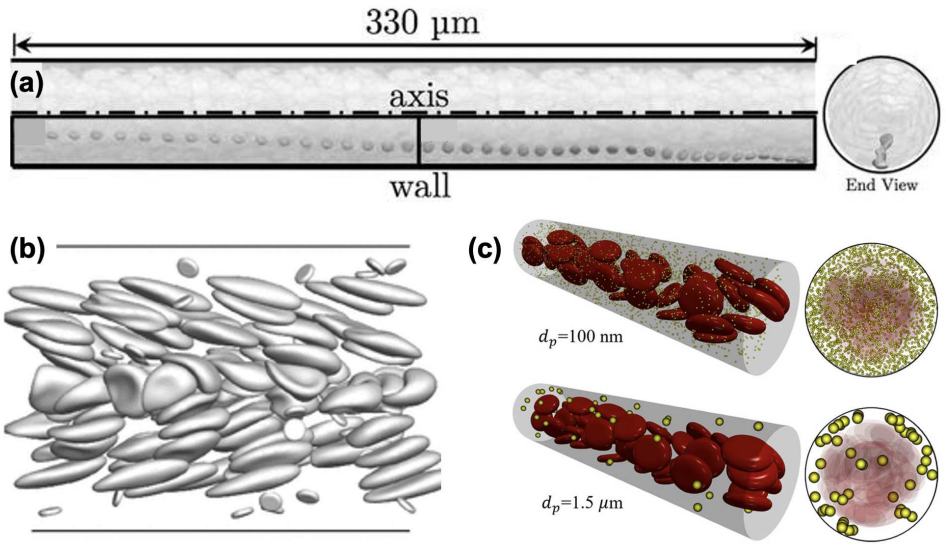

Figure 1. (**a**) Platelet imagination in a 3-D microvessel (adapted with permission from Reasor et al. [25]). (**b**) Snapshots of platelet imagination and flipping near the wall in a 2-D channel flow (adapted with permission from Zhao and Shaqfeh [26]). (**c**) Margination occurs only for microscale particles, not for nanoscale particles. (adapted with permission from Liu et al. [31])

3. Platelet Adhesion

Platelet adhesion to the vessel wall is primarily mediated by VWF and fibrinogen, two of the most physiologically relevant ligands that support thrombosis and hemostasis [33]. Platelet adhesion to fibrinogen is through the binding of integrin $\alpha_{IIb}\beta_3$ to fibrinogen molecules, while adhesion to VWF is through the binding of platelet receptor GPIbα to the VWF-A1 domain. While both support platelet adhesion, the two ligand-receptor pairs show distinct biomechanistic characteristics. As shown by Savage et al. [34,35], $\alpha_{IIb}\beta_3$-fibrinogen binding is effective at wall shear rates of 50 - 500 s^{-1}, while the GPIbα-VWF A1 binding can support pathologically high shear rates above 6000 s^{-1}. In addition, $\alpha_{IIb}\beta_3$-fibrinogen binding relies on platelet activation and can be irreversible, while GPIbα-VWF A1 binding is reversible and independent of platelet activation [36]. Unlike fibrinogen, VWF is a multimer polymer chain that can elongate to expose hundreds of binding sites and extend to tens to hundreds of microns, further enhancing binding events through multivalency. The disparate length scales of all the molecular and cellular players pertinent to platelet binding/adhesion are summarized and highlighted in Figure 2a.

3.1. Binding Kinetics Supporting Platelet Adhesion

Single-molecule experimental assays have enabled direct measurement of platelet binding kinetic rates. Fu et al. [37] measured the apparent on rates of GPIbα-VWF A1 to be above 10^6 $M^{-1}s^{-1}$ using fluorescence single-molecule microscopy. Their measurement is consistent with the earlier work by Wellings and Ku[38], where the GPIbα-VWF A1 bond on (formation) rate is estimated to range from 10^5-10^9 $M^{-1}s^{-1}$ to support firm platelet adhesion under elevated high shear. Combining apparent on rates measurements and kinetic theory, Liu et al. [7] derived the intrinsic on-rate of GPIbα-VWF A1 to be around 10^5 s^{-1}, which means it only takes $\sim$10 μs to form a single bond as long as GPIbα and VWF A1 molecules are sufficiently close. In contrast, the binding of fibrinogen to eptifibatide-primed $\alpha_{IIb}\beta_3$ exhibits an on rate of $\sim 10^4$ $M^{-1}s^{-1}$ [39], which is approximately two orders of magnitude lower than the GPIbα-VWF A1 on rates. Besides on rates, the off rates, the reciprocal of bond lifetime, of GPIbα-VWF A1 and $\alpha_{IIb}\beta_3$-fibrinogen bonds have also been measured [40–42] to be 1 - 100 $^{-1}$, where higher loading forces lead to higher off rates (i.e., shorter bond lifetime). Therefore, the superior effectiveness of the GPIbα-VWF A1 bond compared to the $\alpha_{IIb}\beta_3$-fibrinogen bond for high shear platelet attachment is attributed to the ultra-high on-rates of GPIbα-VWF A1 bond that can form within $\sim$10 μs.

 doi:10.20944/preprints202402.0799.v1

3.2. Multiscale Modelling of Platelet Adhesion

Computational models have been developed to elucidate the rate and pattern of platelet adhesion dynamics. Pioneered by Hammer et al. [43,44], earlier work focused on single-cell adhesion dynamics. Mody et al. [45] established a 2D analytical model and studied the motion pattern of flipping and adhering platelets. Wang et al. [46] utilized a DPD-based model combined with a modified Morse potential (simulating non-bonded electrostatic interactions) to study shear-mediated platelet flipping and adhesion onto an effective VWF surface, showing good correlation with their microchannel perfusion experiments of platelet flipping motion in physiological flow conditions (Figure 2c). While these models can capture the platelet dynamics influenced by the platelet discoid shape and shear transport, they often simplify the effect of molecule components (especially the ligands) through effective kinetics modelling.

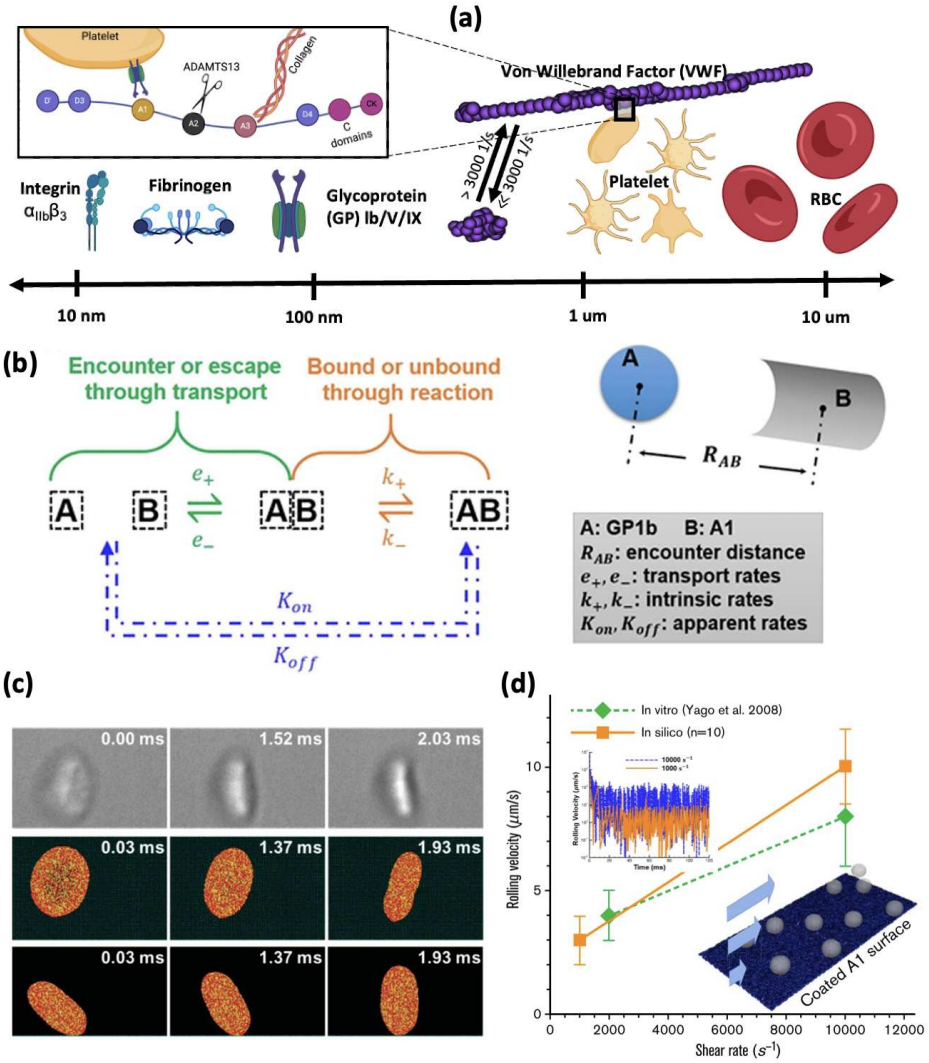

Figure 2. (**a**) Cellular and molecular components related to platelet adhesion ranging from nano (nm) to micron (μm) scales (created with BioRender.com). (**b**) Binding kinetics of GP1b-VWF A1 in flow can be decoupled into a transport and reaction components (adapted with permission from Liu et al. 2021 [7]). (**c**) Snapshots of single platelet flipping motion correlating with in vitro observations (adapted with permission from Wang et al. 2023 [46]). (**d**) Platelet rolling velocity measured based on a multiscale computational model built incorporating molecular and cellular components and their binding kinetics (adapted with permission from Liu et al. 2022 [3])

 doi:10.20944/preprints202402.0799.v1

More recently, multiscale models have been developed to explicitly incorporate molecular components and cellular information. Liu et al. [7] proposed a first principles-based computational model to simulate platelet adhesion to VWF multimers. The model captures the VWF conformational change and the corresponding platelet dynamics under various shear rates. Moreover, they developed a stochastic binding model based on transport-independent intrinsic rates derived from single-molecule kinetics measurements and classical kinetic theory (Figure 2b). Since the model is built from a bottom-up approach, no empirical tuning was found to be necessary to match existing experiments. This was confirmed by platelet rolling velocity captured by the in silico model matching well with the in vitro results shown in Figure 2d [3]. Recently, Belyaev et al. [47] also developed a similar model, where GPIbα-VWF A1 binding was modeled through Morse potential with model parameters tuned to match a specific set of experiments.

4. Platelet Activation

Platelet activation is defined by morphological and structural changes, membrane phospholipid scrambling and procoagulant activity, activation of surface integrins, initiation of internal signaling pathways, granular secretion, and signaling between surface receptors and ligands that lead to adhesion and aggregation [48–50]. Platelet activation can occur after adhesion to the injured endothelial wall or growing thrombus, requires soluble agonists [51], high fluid shear exposure for extended durations, and interaction of GPIbα with VWF immobilized on the damaged blood vessel wall [52] to initiate mechanotransduction effects. Platelet activation can also occur in pathological stenosis or blood-recirculating cardiovascular devices through shear-induced platelet activation (SIPAct) even with little agonist stimulation [50,53,54].

4.1. Platelet Mechanotransduction under Flow Shear Stress

Platelet function in response to fluid shear stress has been extensively studied for a few decades [55–57]. Most approaches have identified the GPIbα-A1 interaction under flow conditions as the primary driver of mechanotransduction [58], where mechanical cues from the surrounding environment are transmitted through the rolling platelet (Figure 3a) and result in structural and biochemical changes. Under pathological high shear flows (i.e., severe stenosis) or elevated high shear conditions in blood-contacting devices (e.g., in left ventricular assist devices), platelet activation can also be mechanically augmented with limited GPIbα-A1 interactions seeing the presence of VWF cleavage [53,59,60]. These mechanical mechanisms of SIPAct may include additive membrane damage (or stress accumulation) [61,62], activation of shear-sensitive channels and pores such as Piezo1 and Pannexin-1 (Panx1) [63–65], and outside-in signaling via a range of transducers other than GPIbα and GPIIb-IIIa (integrin $\alpha_{IIb}\beta_3$) [54,66]. Piezo1 is a mechanosensitive Ca^{2+} permeable cation channel that may contribute to thrombus formation by promoting Ca^{2+} influx under arterial shear [65], senses supraphysiological flow gradients that generate extensional strain leading to deformation in the platelet structure [67](Figure 3b), and upregulates $\alpha_{IIb}\beta_3$ signaling and promotes aggregation in hypertensive mice [68]. Panx1 amplifies the Ca^{2+} signal from Piezo1 to P2X channels [67]. Platelets adhered to a growing thrombus undergo sustained calcium oscillations, in turn inducing a rapid increase in calcium flux in freely translocating platelets tethered to adherent platelets [11].

Phosphoinositide 3-kinase (PI3K) functions as a hub in mechanotransduction and plays a pivotal role in mechanosensing tension, stretching, and compression of the plasma membrane in a variety of cell types [69]. The PI3K/Akt signaling pathway plays a critical role in platelet mechanotransduction [70], regulating VWF A1-GPIbα interaction, intracellular calcium mobilization, $\alpha_{IIb}\beta_3$ activation, adhesion, and thrombus growth [71](Figure 3c). PI3K generates 3-phosphoinositides, involved in all contexts of platelet activation and integrin function [72], and is a critical transmitter of multiple signaling pathways activated by receptor tyrosine kinases (RTK), G-protein coupled receptors (GPCRs), glycoproteins and integrins [73]. The Class I PI3K p110β isoform, which plays a prominent role in structural modelling and motility, has been identified as a potential antithrombotic therapy target [74],

 doi:10.20944/preprints202402.0799.v1

and while it is not required for thrombus growth under physiological conditions, it is necessary for thrombus stability at high shear stress [75]. The PI3K C2α isoform has been identified as essential for Piezo1 activation and may participate by stiffening the cortical cytoskeleton that resists platelet deformation or altering the lipid bilayer membrane composition [67]. Altering platelet mechanical stiffness can also reduce platelet activation under elevated high shear [54].

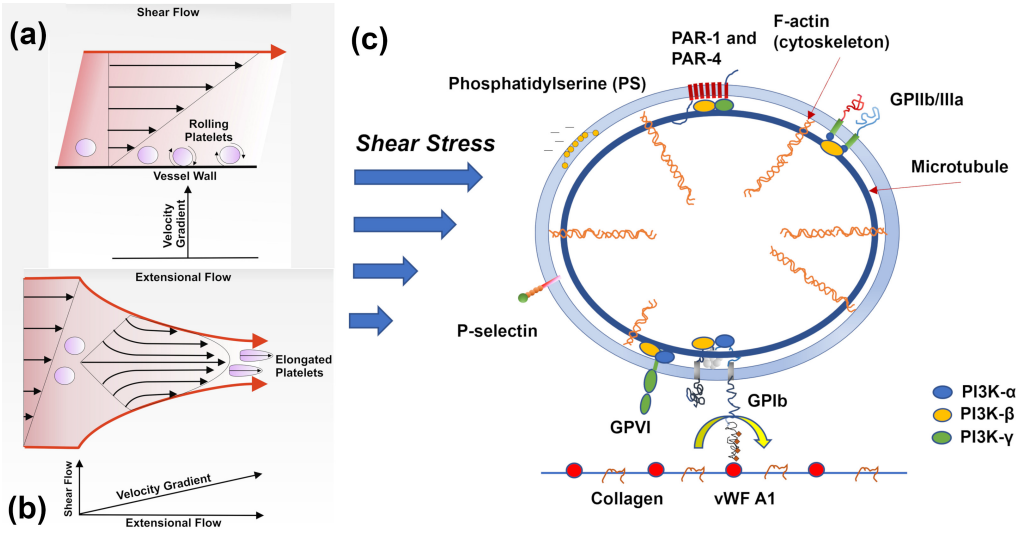

Figure 3. (**a**) Platelets experience wall shear stress as move through layers of the flowing blood and roll along the blood vessel wall (adapted with permission from Zainal Abidin et al. 2023 [76]). (**b**) Platelets elongate as they experience extensional stresses due to fluid acceleration parallel to the wall, particularly in areas of stenoses (adapted with permission from Zainal Abidin et al. 2023 [76]). (**c**) Upstream and downstream participants are involved in shear-mediated platelet mechanotransduction, with PI3K as the primary driver.

4.2. Resting and Activated Platelet Morphology under Flow Conditions

Resting or quiescent platelets are generally approximated as oblate spheroids [77], particularly for computational hydrodynamics models [78,79]. Submembrane cortical structural elements involved in shear-induced platelet activation include actin, myosin, spectrin and intermediate filaments [80], providing tension to the platelet surface and allowing the lipid bilayer membrane to "wrinkle" [81]. During activation and spreading, the bilayer unfolds to a larger surface area and provides a buffer for changes in surface membrane tension, effectively dampening platelet activation resulting from rapid blood flow fluctuations [82]. The microtubule marginal band generates the platelet discoid structure and consists of dynamic microtubules [83,84]. When the platelet is activated, the microtubule coil disassembles and reduces in diameter [84] and plays a diminished role in platelet function [85]. The actin cytoskeleton supports the platelet's discoid structure and actively aids in platelet spreading [86]. Compressed spectrin-rich networks sandwiched between the membrane and cytoskeleton intersperse GPIb-IX-actin binding protein complexes connected to filamentous actin (F-actin) radially projecting from a central cross-linked F-actin core [86]. Upon activation, soluble F-actin polymerizes into an average of 2,000 filaments, each approximately 1.1 μm long, promoting the formation of platelet pseudopods [86]. Upon activation, actin is fragmented, and the platelet assumes a spherical form [80]. The spectrin network then swells and allows the protrusion of spindle-like filopods or sheet-like lamellipods with additional actinassembling signals [87].

Under pathological flow conditions, such as those found in arterial stenoses, platelets transform into spherical shapes, show extended pseudopods, and have occasional organelle centralization [88]. Integrin $\alpha_{IIb}\beta_3$ receptors redistribute and relocate to the pseudopod extremities, but platelets remain in a state of reversible activation [88]. Platelets in stroke patients show significant cytoskeletal rearrangement [89]. Under hypershear conditions, platelets exhibit more dramatic shape change, with

 doi:10.20944/preprints202402.0799.v1

some platelets exhibiting severe damage characterized by leaky membranes and total breakdown of the microtubule band and actin cytoskeleton [90,91]. Membrane stretching associated with elongational stresses in the descending aorta during diastole may allow a conformational change in the platelet receptors, increasing ligand binding affinity and allowing increased ion permeability [92]. Hypershear stresses and short exposure times found in cardiovascular devices such as ventricular assist devices promote $\alpha_{IIb}\beta_3$, GPIbα, and GPVI receptor shedding, additionally promoting bleeding complications [93–95], and procoagulant microparticles are formed and released from the platelet surface [96].

4.3. Changes in Platelet Mechanobiology due to Aging

Studies limited to an upper age of 65 have observed age-related differences in platelet function, showing increasing trends in ADP- and collagen-induced aggregation [97] and stability in VWF-triggered adhesion with age [98]. The elderly exhibit increasingly activated platelets that lose their full aggregation potential [99]. In contrast, platelets from newborns are traditionally hypoactive [100], with impaired calcium mobilization [101], agonist-induced aggregation [102], and surface receptor expression [103], but similar agonist-induced thrombin generation [104–106] and flow-induced adhesion to VWF and collagen as adult platelets [107,108]. Umbilical cord platelets exposed to fluid shear have similar membrane phosphatidylserine and prothrombinase activity as adult platelets, but this behavior is uniquely calcium-independent [109]. Neonatal platelets have under-expressed genes regulating the actin cytoskeleton and cell signaling [110], and have a less developed tubular structure [111]. Still, very little is known about platelet structural and functional changes in the elderly or young, as most research is still performed on volunteers aged 18-65, calling for more studies to focus on older or pediatric individuals to draw more conclusions regarding aging dependence of platelet activation and function [97].

4.4. Multiscale Modelling of Shear-induced Platelet Activation

Early multiscale models of shear-induced platelet activation simplified platelets as an ensemble of bound particles with an enclosing membrane or continuous solid resembling a rigid ellipsoid shape, neglecting molecular intraplatelet constituents and membrane deformability [45,112–116]. Two of these early models were adapted to include subcellular elements (SCE) [116,117] to represent the cytoskeletal network and continuum description of the lipid bilayer, thereby enabling modelling of platelet motion and deformation in flowing blood, described by a lattice-Boltzmann approach, as well as variability in the platelet stiffness [117]. Zhang et al. [118] developed a coupled approach where DPD describes the top-scale viscous fluid flow. The bottom-scale deformable platelet utilizes a CGMD approach to build a molecular model of platelets (Figure 4a). This CGMD model consists of approximately 140,000 particles representing viscoelastic bilayer membrane, functional actin cytoskeleton consisting of α-helix filaments, supporting actin core, and cytoplasm. The particles interact using bonded spring forces and non-bonded Lennard-Jones electrostatic potentials [118,119]. Using this approach, Pothapragada simulated platelet shape change and filopodia formation under shear stresses up to 70 dyne/cm^2, in good agreement with in vitro experiments (Figure 4c) [120]. Zhang et al. showed that this model allows regional mapping of hemodynamic stresses encountered in flowing blood to the bilayer membrane and actin cytoskeletal structure, thereby identifying locations on and within the platelet likely to undergo mechanotransduction (Figure 4b) [119], as well as predict locations where filopodia are likely to form [121]. The platelet CGMD model was updated to include the microtubule function, where extension of filopodia are anchored at the filamentous core and allowed to coil around the submembrane platelet periphery as filopodia protrude from the platelet [121].

 doi:10.20944/preprints202402.0799.v1

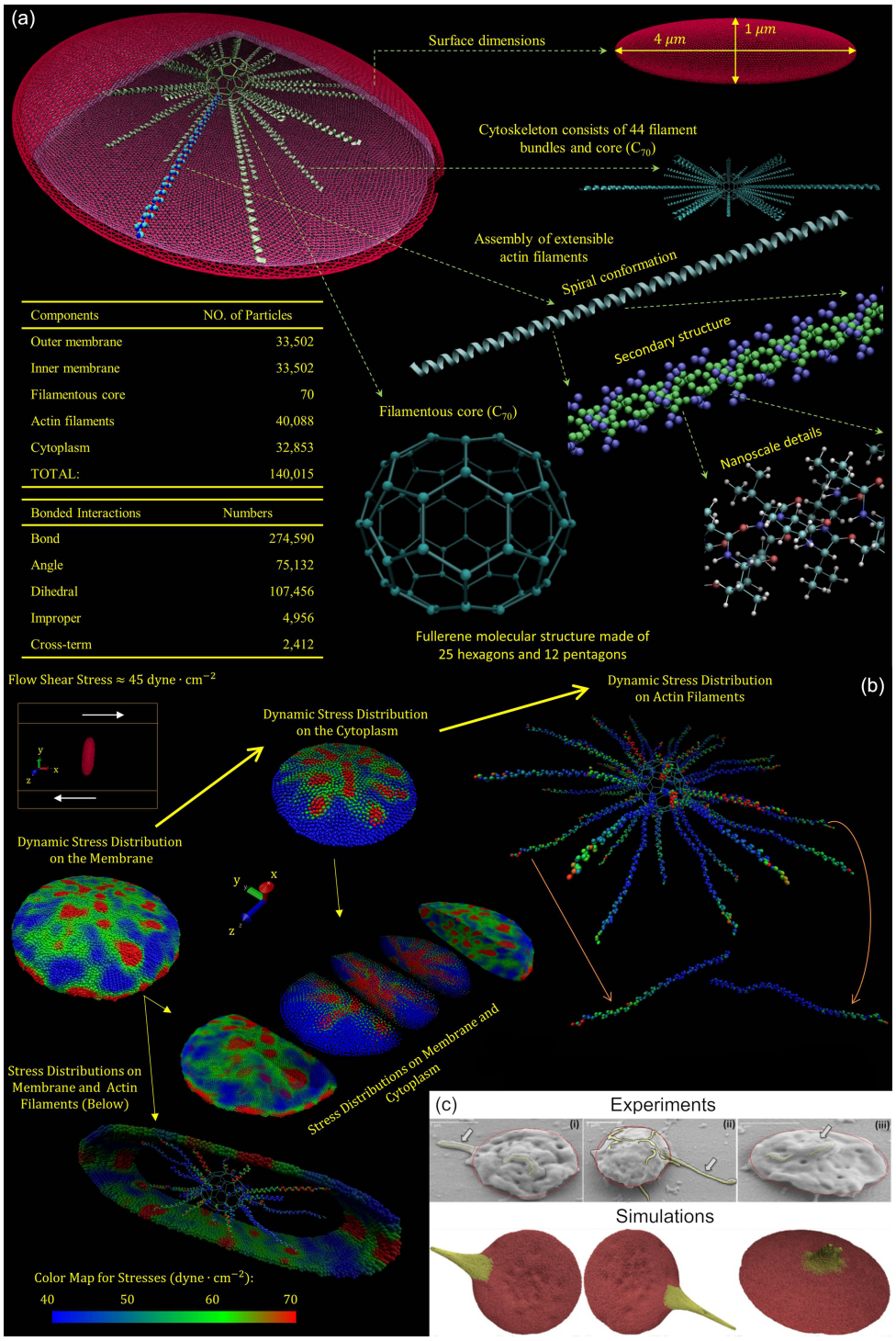

Figure 4. (**a**) Coarse-grained molecular dynamics model of the intracellular constituent structure of human platelets (Reprinted with permission from Zhang et al., 2017 [119]). (**b**) Stress distributions on the platelet membrane, cytoplasm, and actin cytoskeleton (Adapted with permission from Zhang et al., 2017 [119]). (**c**) Visual comparison of experimental and simulated filopodia formation: (**i**) scanning image after exposure to 1 dyne/cm^2 for 4 min, (**ii**) 70 dyne/cm^2 for 4 min, and (**iii**) 70 dyne/cm^2 for 1 min (adapted with permission from Pothapragada et al., 2015 [120])

 doi:10.20944/preprints202402.0799.v1

5. Platelet Aggregation

Platelet aggregation can be supported through different pathways depending on the levels of shear rates [6,122], as demonstrated in Figure 5a. At low shear rates (100 to 1000 s^{-1}), platelet aggregation relies on platelet activation as a prerequisite to activate the integrin $\alpha_{IIb}\beta_3$ adhesion to fibrinogen [6,34,35,122,123] supported by platelet morphological change, such as sphere and filopodia. At physiologically high shear rates (1000 to 10 000 s^{-1}), a two-stage aggregation process is observed, where unstable clusters of discoid platelets facilitated by membrane tethers and GPIbα-VWF A1 become converted to stable aggregates through platelet activation and mechanotransduction, forming irreversible $\alpha_{IIb}\beta_3$-fibrinogen bonds [6,122]. At pathologically high shear conditions (> 10,000 s^{-1}), platelet aggregation can be initiated independently of platelet activation, with VWF-GPIbα-VWF bonds being the sole mediator [6,7,36,122]. At these elevated shear rates, platelets change their shape to a smooth, spherical shape [3,6]. Overall, the increase in shear rate leads to more VWF-mediated binding and less platelet activation-induced binding.

5.1. Multiscale Modelling of Shear-induced Platelet Aggregation

Computational models have been developed to understand platelet aggregation in all three shear regimes. More comprehensive reviews of platelet aggregation modelling can be found in Fogelson and Neeves [124] and Kim et al. [5]. We highlight a few studies for the three shear regimes as indicated in Figure 5a.

For low shear regimes (100 to 1000 s^{-1}), Flamm et al. [125] developed a patient-specific model for platelet aggregation in flow. A neural network (NN) model of calcium regulation was trained on patient data and integrated into the model to provide a donor-specific prediction of platelet response in flow. Gupta et al. [126,127] developed a multiscale model combining dissipative particle dynamics and coarse-grained molecular dynamics to simulate the aggregation of free-flowing platelets, where the aggregation is driven by the interaction of $\alpha_{IIb}\beta_3$ receptors and fibrinogen (Figure 5b). Generally, these models neglect morphological changes such as activated platelet filopodia formation, which could enhance the aggregation through increased contact area as reported in Maxwell et al. [122].

For the physiologically high shear regime (1000 to 10,000 s^{-1}), Fogelson and Guy [128] studied platelet aggregation at a shear rate of 1750 s^{-1} using immersed-boundary type methods. Using this approach, they observe platelets accumulate as mural aggregates after agonist-induced platelet activation. Mori et al. [129] developed a Stokesian Dynamics model to simulate platelet binding with fibrinogen and VWF concurrently under a shear rate of 5000 s^{-1}. They found both $\alpha_{IIb}\beta_3$-fibrinogen and GPIbα-VWF A1 bonds are necessary to form stable aggregates in this shear regime. Shankar et al. applied a multiscale computational method to simulate thrombus growth across a shear range of 100∼8000 s^{-1} [130], showing the necessity of considering the VWF-mediated platelet aggregation to form occlusion under high shear (Figure 5c). In these models, the receptor-ligand and their molecular kinetics were not modeled directly; instead, adhesion was provided by elastic links between immersed boundary points both on the platelet and the wall.

For the pathologically high shear regime (>10,000 s^{-1}) relevant to acute occlusive arterial thrombosis, Liu et al. [3,7] recently developed a multiscale computational model that integrates VWF multimers, inactivated platelets, and GPIbα-VWF A1 binding kinetics based on experimental measurements to unravel the dynamic process of shear-induced platelet aggregation, shown in Figure 5d. Their model predicts that the aggregation process can occur in less than 10 milliseconds, potentially explaining how billions of platelets can be captured in less than 10 minutes when they pass through arterial stenosis to form an occlusive thrombus. Recently, Du et al. [131], Du and Fogelson [132] developed a continuum model to study occlusive arterial thrombosis formation in a stenosis. Their model confirmed experimental observations that VWF is a necessary ingredient to form occlusive clots under elevated high shear rates.

 doi:10.20944/preprints202402.0799.v1

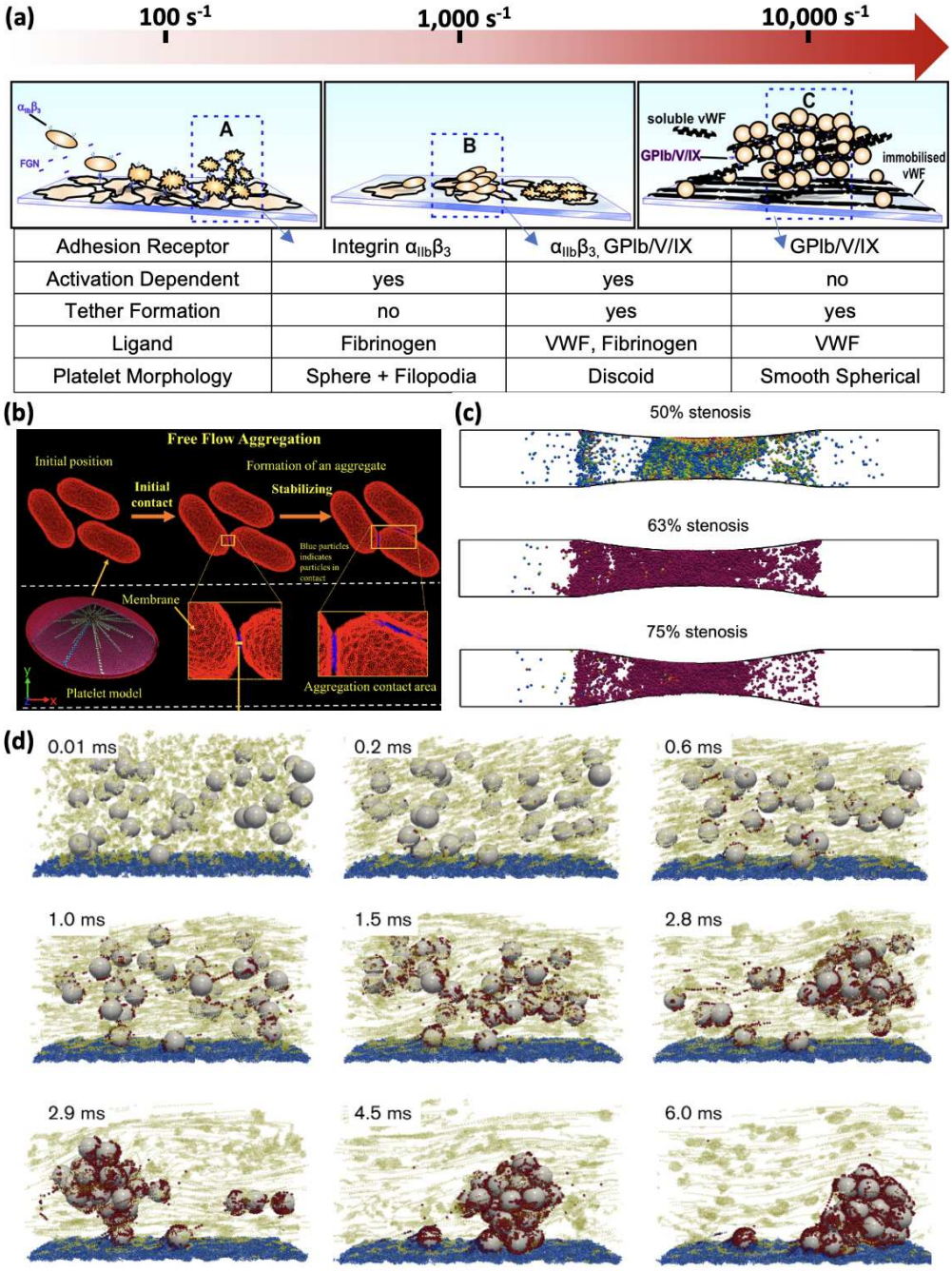

Adhesion Receptor	Integrin $\alpha_{IIb}\beta_3$	$\alpha_{IIb}\beta_3$, GPIb/V/IX	GPIb/V/IX
Activation Dependent	yes	yes	no
Tether Formation	no	yes	yes
Ligand	Fibrinogen	VWF, Fibrinogen	VWF
Platelet Morphology	Sphere + Filopodia	Discoid	Smooth Spherical

Figure 5. (**a**) Different pathways of platelet aggregation under various levels of shear rates. (adapted with permission from Maxwell et al. [133]). (**b**) Simulated aggregation of three adjacent platelets through a DPD-CGMD coupled multiscale method. (adapted with permission from Gupta et al. [127]). (**c**) Snapshots of platelet aggregate formation at the wall induced by agonist-induced platelet activation (adapted with permission from Shankar et al. [130]). (**d**) Activation-independent platelet aggregation occurs in less than 10 ms (adapted with permission from Liu et al. [3]).

6. Platelet Mechanobiology Modelling in the Age of Data

Artificial Intelligence (AI) techniques have recently been used to study platelet mechanobiology. Chatterjee et al. used a pairwise agonist scanning approach to measure intracellular Ca^{2+} level for platelet-rich plasma treated with six agonists, which was then used to train a neural network model to accurately predict time-course traces of Ca^{2+} increase [134]. Using a convolutional neural network

 doi:10.20944/preprints202402.0799.v1

(CNN) to identify subtle morphological features, Zhou et al. classified platelet aggregates activated by different agonists [135], while Kempster et al. used a CNN to automate analysis of spreading platelets captured under differential interference contrast (DIC) microscopy [136]. Semi-unsupervised learning based on CNN has been used to categorize morphology from platelets dynamics in microchannels [46,137–139]. Several researchers have attempted to classify cellular information using features from diverse data types. These approaches combine models and datasets vertically across spatial and temporal scales or horizontally at a particular scale. They are useful for predicting labels of individual entities, such as gene function, or relationships, such as functional associations or causal relationships between biomedical entities [140]. Shankar et al. [141] integrated the platelet signaling NN module developed by Chatterjee et al. [134] into a 3D multiscale framework predicting thrombus growth on the surface containing both tissue factor and collagen. AI-aided time-stepping algorithms have also been used to speed up multiscale simulations while maintaining good spatiotemporal resolutions [142,143].

7. Summary

Thrombosis is a complex biorheological and mechanobiological process spanning multiple spatial and temporal scales. Under pathological flow conditions, the platelet marginates towards an injured vessel or device wall, with which it adheres through receptor-ligand interactions. The thrombus grows as flowing platelets aggregate and get captured at the wall. During these phases of thrombosis, platelets encounter molecular ligands (such as VWF) in the presence of fluid shear forces. Platelets may also activate through a mechanotransduction process given sufficient time under specific stress levels. Further complexity arises from the effect of aging on platelet mechanobiology. While these phenomena have been extensively studied in vitro and in vivo, computational biology approaches, as we have described, have become more efficient at probing the intricacies of thrombosis and elucidating the link between molecular level kinetics and platelet mechanotransductive mechanisms in a growing clot, with advances in replicating platelet mechanobiology. The growing role of artificial intelligence and its integration with computational biology holds the promise of enhancing both benchtop and computational approaches for characterizing and predicting multiscale thrombosis events as a paradigm of digital medicine.

Author Contributions: Conceptualization, R.T., Z.L.L., and J.S.; Writing – Original Draft Preparation, R.T., Y.D., D.B., W.Y. Z.L.L., and J.S.; Writing – Review and Editing, R.T., W.Y., E.C.C, J.R., Y.D., D.B., Y.R., J.J.G., Y.L., Z.L.L., and J.S.; Visualization, R.T., Z.L.L, and J.S.

Funding: This research received no external funding.

Informed Consent Statement: Not applicable.

Acknowledgments: The authors gratefully acknowledge the authors and publishers who allowed reuse of some of the original figures for this review.

Conflicts of Interest: The authors declare no conflict of interest.

References

1. Watson, T.; Shantsila, E.; Lip, G.Y. Mechanisms of thrombogenesis in atrial fibrillation: Virchow's triad revisited. *The Lancet* **2009**, *373*, 155–166.
2. Casa, L.D.; Deaton, D.H.; Ku, D.N. Role of high shear rate in thrombosis. *Journal of vascular surgery* **2015**, *61*, 1068–1080.
3. Liu, Z.L.; Bresette, C.; Aidun, C.K.; Ku, D.N. SIPA in 10 milliseconds: VWF tentacles agglomerate and capture platelets under high shear. *Blood Advances* **2022**, *6*, 2453–2465.
4. Casa, L.D.; Ku, D.N. Thrombus Formation at High Shear Rates. *Annu. Rev. Biomed. Eng.* **2017**, *19*, 415–433.
5. Kim, D.; Bresette, C.; Liu, Z.; Ku, D.N. Occlusive thrombosis in arteries. *APL bioengineering* **2019**, *3*.
6. Jackson, S.P. The growing complexity of platelet aggregation. *Blood, The Journal of the American Society of Hematology* **2007**, *109*, 5087–5095.
7. Liu, Z.L.; Ku, D.N.; Aidun, C.K. Mechanobiology of shear-induced platelet aggregation leading to occlusive arterial thrombosis: A multiscale in silico analysis. *Journal of Biomechanics* **2021**, *120*, 110349.

 doi:10.20944/preprints202402.0799.v1

8. Chow, T.W.; Hellums, J.D.; Moake, J.L.; Kroll, M.H. Shear stress-induced von Willebrand factor binding to platelet glycoprotein Ib initiates calcium influx associated with aggregation. *Blood* **1992**, *80*, 113–20.
9. Jackson, S.; Nesbitt, W.; Westein, E. Dynamics of platelet thrombus formation. *Journal of Thrombosis and Haemostasis* **2009**, *7*, 17–20.
10. Moake, J.L.; Turner, N.A.; Stathopoulos, N.A.; Nolasco, L.H.; Hellums, J.D. Involvement of large plasma von Willebrand factor (vWF) multimers and unusually large vWF forms derived from endothelial cells in shear stress-induced platelet aggregation. *The Journal of clinical investigation* **1986**, *78*, 1456–1461.
11. Ruggeri, Z.M. Platelet Adhesion under Flow. *Microcirculation* **2009**, *16*, 58–83.
12. Shiozaki, S.; Takagi, S.; Goto, S. Prediction of molecular interaction between platelet glycoprotein Ibα and von Willebrand factor using molecular dynamics simulations. *Journal of atherosclerosis and thrombosis* **2016**, *23*, 455–464.
13. Tong, D.; Soley, N.; Kolasangiani, R.; Schwartz, M.A.; Bidone, T.C. Integrin αIIbβ3 intermediates: From molecular dynamics to adhesion assembly. *Biophysical Journal* **2023**, *122*, 533–543.
14. Aidun, C.K.; Clausen, J.R. Lattice-Boltzmann method for complex flows. *Annual review of fluid mechanics* **2010**, *42*, 439–472.
15. Groot, R.D.; Warren, P.B. Dissipative particle dynamics: Bridging the gap between atomistic and mesoscopic simulation. *The Journal of chemical physics* **1997**, *107*, 4423–4435.
16. Dzwinel, W.; Yuen, D.A.; Boryczko, K. Mesoscopic dynamics of colloids simulated with dissipative particle dynamics and fluid particle model. *Molecular modeling annual* **2002**, *8*, 33–43.
17. Dzwinel, W.; Boryczko, K.; Yuen, D.A. A discrete-particle model of blood dynamics in capillary vessels. *Journal of colloid and interface science* **2003**, *258*, 163–173.
18. N'dri, N.A.; Shyy, W.; Tran-Son-Tay, R. Computational modeling of cell adhesion and movement using a continuum-kinetics approach. *Biophysical journal* **2003**, *85*, 2273–2286.
19. Shyy and, W.; Francois, M.; Udaykumar, H.S.; N'dri and, N.; Tran-Son-Tay, R. Moving boundaries in micro-scale biofluid dynamics. *Appl. Mech. Rev.* **2001**, *54*, 405–454.
20. Rao, R.R.; Clausen, J.; Roberts, S.A.; Lechman, J.B.; Wagner, J.; Butler, K.; Bolintineanu, D.; Brinker, C.J.; Liu, L. Continuum modeling of Nanoparticle Transport in the Vasculature. Technical report, Sandia National Lab.(SNL-NM), Albuquerque, NM (United States), 2017.
21. Rao, R.R.; Wagner, J.; Butler, K.; Clausen, J.; Martin, R.M.; Liu, L. Continuum Modeling of Nanoparticles Transport In Vivo Through Bifurcations. Technical report, Sandia National Lab.(SNL-NM), Albuquerque, NM (United States), 2018.
22. Mehrabadi, M.; Ku, D.N.; Aidun, C.K. Effects of shear rate, confinement, and particle parameters on margination in blood flow. *Phys. Rev. E* **2016**, *93*, 023109.
23. Crowl, L.; Fogelson, A.L. Analysis of mechanisms for platelet near-wall excess under arterial blood flow conditions. *Journal of fluid mechanics* **2011**, *676*, 348–375.
24. Aarts, P.A.; van den Broek, S.A.; Prins, G.W.; Kuiken, G.D.; Sixma, J.J.; Heethaar, R.M. Blood platelets are concentrated near the wall and red blood cells, in the center in flowing blood. *Arteriosclerosis (Dallas, Tex.)* **1988**, *8*, 819–824. Place: United States Publisher: Am Heart Assoc.
25. Reasor, D.A.; Mehrabadi, M.; Ku, D.N.; Aidun, C.K. Determination of Critical Parameters in Platelet Margination. *Ann Biomed Eng* **2013**, *41*, 238–249.
26. Zhao, H.; Shaqfeh, E.S. Shear-induced platelet margination in a microchannel. *Physical Review E* **2011**, *83*, 061924.
27. Zhao, H.; Shaqfeh, E.S.; Narsimhan, V. Shear-induced particle migration and margination in a cellular suspension. *Physics of Fluids* **2012**, *24*.
28. Kumar, A.; Graham, M.D. Margination and segregation in confined flows of blood and other multicomponent suspensions. *Soft Matter* **2012**, *8*, 10536–10548.
29. Kumar, A.; Graham, M.D. Mechanism of Margination in Confined Flows of Blood and Other Multicomponent Suspensions. *Phys. Rev. Lett.* **2012**, *109*, 108102.
30. Liu, Z.; Zhu, Y.; Clausen, J.R.; Lechman, J.B.; Rao, R.R.; Aidun, C.K. Multiscale method based on coupled lattice-Boltzmann and Langevin-dynamics for direct simulation of nanoscale particle/polymer suspensions in complex flows. *International Journal for Numerical Methods in Fluids* **2019**, *91*, 228–246.
31. Liu, Z.; Clausen, J.R.; Rao, R.R.; Aidun, C.K. A unified analysis of nano-to-microscale particle dispersion in tubular blood flow. *Physics of Fluids* **2019**, *31*.
32. Liu, Z.; Clausen, J.R.; Rao, R.R.; Aidun, C.K. Nanoparticle diffusion in sheared cellular blood flow. *Journal of Fluid Mechanics* **2019**, *871*, 636–667.

 doi:10.20944/preprints202402.0799.v1

33. Ruggeri, Z.M.; Mendolicchio, G.L. Adhesion Mechanisms in Platelet Function. *Circulation Research* **2007**, *100*, 1673–1685.
34. Savage, B.; Saldívar, E.; Ruggeri, Z.M. Initiation of platelet adhesion by arrest onto fibrinogen or translocation on von Willebrand factor. *Cell* **1996**, *84*, 289–297.
35. Savage, B.; Almus-Jacobs, F.; Ruggeri, Z.M. Specific synergy of multiple substrate–receptor interactions in platelet thrombus formation under flow. *Cell* **1998**, *94*, 657–666.
36. Ruggeri, Z.M.; Orje, J.N.; Habermann, R.; Federici, A.B.; Reininger, A.J. Activation-independent platelet adhesion and aggregation under elevated shear stress. *Blood* **2006**, *108*, 1903–1910.
37. Fu, H.; Jiang, Y.; Yang, D.; Scheiflinger, F.; Wong, W.P.; Springer, T.A. Flow-induced elongation of von Willebrand factor precedes tension-dependent activation. *Nature communications* **2017**, *8*, 324.
38. Wellings, P.J.; Ku, D.N. Mechanisms of Platelet Capture Under Very High Shear. *Cardiovasc Eng Tech* **2012**, *3*, 161–170.
39. Hantgan, R.R.; Stahle, M.C.; Lord, S.T. Dynamic Regulation of Fibrinogen: Integrin αIIbβ3 Binding. *Biochemistry* **2010**, *49*, 9217–9225.
40. Yago, T.; Lou, J.; Wu, T.; Yang, J.; Miner, J.J.; Coburn, L.; López, J.A.; Cruz, M.A.; Dong, J.F.; McIntire, L.V. Platelet glycoprotein Ibα forms catch bonds with human WT vWF but not with type 2B von Willebrand disease vWF. *The Journal of clinical investigation* **2008**, *118*, 3195–3207.
41. Chen, Y.; Liao, J.; Yuan, Z.; Li, K.; Liu, B.; Ju, L.A.; Zhu, C. Fast force loading disrupts molecular binding stability in human and mouse cell adhesions. *Molecular & cellular biomechanics: MCB* **2019**, *16*, 211.
42. Chen, Y.; Ju, L.A.; Zhou, F.; Liao, J.; Xue, L.; Su, Q.P.; Jin, D.; Yuan, Y.; Lu, H.; Jackson, S.P. An integrin αIIbβ3 intermediate affinity state mediates biomechanical platelet aggregation. *Nature materials* **2019**, *18*, 760–769.
43. Hammer, D.A.; Lauffenburger, D.A. A dynamical model for receptor-mediated cell adhesion to surfaces. *Biophysical journal* **1987**, *52*, 475–487.
44. Hammer, D.A.; Apte, S.M. Simulation of cell rolling and adhesion on surfaces in shear flow: general results and analysis of selectin-mediated neutrophil adhesion. *Biophysical journal* **1992**, *63*, 35–57.
45. Mody, N.A.; Lomakin, O.; Doggett, T.A.; Diacovo, T.G.; King, M.R. Mechanics of transient platelet adhesion to von Willebrand factor under flow. *Biophysical journal* **2005**, *88*, 1432–1443.
46. Wang, P.; Sheriff, J.; Zhang, P.; Deng, Y.; Bluestein, D. A Multiscale Model for Shear-Mediated Platelet Adhesion Dynamics: Correlating In Silico with In Vitro Results. *Ann Biomed Eng* **2023**, *51*, 1094–1105.
47. Belyaev, A.V.; Kushchenko, Y.K. Biomechanical activation of blood platelets via adhesion to von Willebrand factor studied with mesoscopic simulations. *Biomech Model Mechanobiol* **2023**, *22*, 785–808.
48. Cosemans, J.M.; Angelillo-Scherrer, A.; Mattheij, N.J.; Heemskerk, J.W. The effects of arterial flow on platelet activation, thrombus growth, and stabilization. *Cardiovascular research* **2013**, *99*, 342–352.
49. Versteeg, H.H.; Heemskerk, J.W.M.; Levi, M.; Reitsma, P.H. New Fundamentals in Hemostasis. *Physiological Reviews* **2013**, *93*, 327–358.
50. Kim, D.A.; Ashworth, K.J.; Di Paola, J.; Ku, D.N. Platelet α-granules are required for occlusive high-shear-rate thrombosis. *Blood advances* **2020**, *4*, 3258–3267.
51. Jennings, L. Mechanisms of platelet activation: Need for new strategies to protect against platelet-mediated atherothrombosis. *Thromb Haemost* **2009**, *102*, 248–257.
52. Kroll, M.H.; Harris, T.S.; Moake, J.L.; Handin, R.I.; Schafer, A.I. von Willebrand factor binding to platelet GpIb initiates signals for platelet activation. *The Journal of clinical investigation* **1991**, *88*, 1568–1573.
53. Meyer, A.L.; Malehsa, D.; Bara, C.; Budde, U.; Slaughter, M.S.; Haverich, A.; Strueber, M. Acquired von Willebrand Syndrome in Patients With an Axial Flow Left Ventricular Assist Device. *Circ: Heart Failure* **2010**, *3*, 675–681.
54. Slepian, M.J.; Sheriff, J.; Hutchinson, M.; Tran, P.; Bajaj, N.; Garcia, J.G.; Saavedra, S.S.; Bluestein, D. Shear-mediated platelet activation in the free flow: Perspectives on the emerging spectrum of cell mechanobiological mechanisms mediating cardiovascular implant thrombosis. *Journal of biomechanics* **2017**, *50*, 20–25.
55. Hellums, J.; Peterson, D.; Stathopoulos, N.; Moake, J.; Giorgio, T. Studies on the mechanisms of shear-induced platelet activation. In Proceedings of the Cerebral ischemia and hemorheology. Springer, 1987, pp. 80–89.
56. Kroll, M.H.; Hellums, J.D.; McIntire, L.V.; Schafer, A.I.; Moake, J.L. Platelets and shear stress. *Blood* **1996**, *88*, 1525–41.
57. Girdhar, G.; Bluestein, D. Biological effects of dynamic shear stress in cardiovascular pathologies and devices. *Expert Review of Medical Devices* **2008**, *5*, 167–181.

 doi:10.20944/preprints202402.0799.v1

58. Ingber, D.E.; Wang, N.; Stamenović, D. Tensegrity, cellular biophysics, and the mechanics of living systems. *Reports on Progress in Physics* **2014**, *77*, 046603.
59. Sheriff, J.; Bluestein, D.; Girdhar, G.; Jesty, J. High-Shear Stress Sensitizes Platelets to Subsequent Low-Shear Conditions. *Ann Biomed Eng* **2010**, *38*, 1442–1450.
60. Sheriff, J.; Tran, P.L.; Hutchinson, M.; DeCook, T.; Slepian, M.J.; Bluestein, D.; Jesty, J. Repetitive Hypershear Activates and Sensitizes Platelets in a Dose-Dependent Manner. *Artificial Organs* **2016**, *40*, 586–595.
61. Girdhar, G.; Xenos, M.; Alemu, Y.; Chiu, W.C.; Lynch, B.E.; Jesty, J.; Einav, S.; Slepian, M.J.; Bluestein, D. Device thrombogenicity emulation: a novel method for optimizing mechanical circulatory support device thromboresistance. *PloS one* **2012**, *7*, e32463.
62. Sheriff, J.; Soares, J.S.; Xenos, M.; Jesty, J.; Bluestein, D. Evaluation of Shear-Induced Platelet Activation Models Under Constant and Dynamic Shear Stress Loading Conditions Relevant to Devices. *Ann Biomed Eng* **2013**, *41*, 1279–1296.
63. Taylor, K.A.; Wright, J.R.; Mahaut-Smith, M.P. Regulation of Pannexin-1 channel activity. *Biochemical Society Transactions* **2015**, *43*, 502–507.
64. Taylor, K.A.; Wright, J.R.; Vial, C.; Evans, R.J.; Mahaut-Smith, M.P. Amplification of human platelet activation by surface pannexin-1 channels. *Journal of Thrombosis and Haemostasis* **2014**, *12*, 987–998.
65. Ilkan, Z.; Wright, J.R.; Goodall, A.H.; Gibbins, J.M.; Jones, C.I.; Mahaut-Smith, M.P. Evidence for shear-mediated Ca2+ entry through mechanosensitive cation channels in human platelets and a megakaryocytic cell line. *Journal of Biological Chemistry* **2017**, *292*, 9204–9217.
66. Mammadova-Bach, E.; Gudermann, T.; Braun, A. Platelet Mechanotransduction: Regulatory Cross Talk Between Mechanosensitive Receptors and Calcium Channels. *ATVB* **2023**, *43*, 1339–1348.
67. Zainal Abidin, N.A.; Poon, E.K.W.; Szydzik, C.; Timofeeva, M.; Akbaridoust, F.; Brazilek, R.J.; Tovar Lopez, F.J.; Ma, X.; Lav, C.; Marusic, I.; et al. An extensional strain sensing mechanosome drives adhesion-independent platelet activation at supraphysiological hemodynamic gradients. *BMC Biol* **2022**, *20*, 73.
68. Zhao, W.; Wei, Z.; Xin, G.; Li, Y.; Yuan, J.; Ming, Y.; Ji, C.; Sun, Q.; Li, S.; Chen, X. Piezo1 initiates platelet hyperreactivity and accelerates thrombosis in hypertension. *Journal of Thrombosis and Haemostasis* **2021**, *19*, 3113–3125.
69. Di-Luoffo, M.; Ben-Meriem, Z.; Lefebvre, P.; Delarue, M.; Guillermet-Guibert, J. PI3K functions as a hub in mechanotransduction. *Trends in Biochemical Sciences* **2021**, *46*, 878–888.
70. Chen, Z.; Li, T.; Kareem, K.; Tran, D.; Griffith, B.P.; Wu, Z.J. The role of PI3K/Akt signaling pathway in non-physiological shear stress-induced platelet activation. *Artificial Organs* **2019**, *43*, 897–908.
71. Yap, C.L.; Anderson, K.E.; Hughan, S.C.; Dopheide, S.M.; Salem, H.H.; Jackson, S.P. Essential role for phosphoinositide 3-kinase in shear-dependent signaling between platelet glycoprotein Ib/V/IX and integrin αIIbβ3. *Blood, The Journal of the American Society of Hematology* **2002**, *99*, 151–158.
72. Guidetti, G.F.; Canobbio, I.; Torti, M. PI3K/Akt in platelet integrin signaling and implications in thrombosis. *Advances in biological regulation* **2015**, *59*, 36–52.
73. Ghigo, A.; Morello, F.; Perino, A.; Hirsch, E. Therapeutic applications of PI3K inhibitors in cardiovascular diseases. *Future Medicinal Chemistry* **2013**, *5*, 479–492.
74. Jackson, S.P.; Schoenwaelder, S.M.; Goncalves, I.; Nesbitt, W.S.; Yap, C.L.; Wright, C.E.; Kenche, V.; Anderson, K.E.; Dopheide, S.M.; Yuan, Y. PI 3-kinase p110β: a new target for antithrombotic therapy. *Nature medicine* **2005**, *11*, 507–514.
75. Laurent, P.A.; Séverin, S.; Hechler, B.; Vanhaesebroeck, B.; Payrastre, B.; Gratacap, M.P. Platelet PI3Kβ and GSK3 regulate thrombus stability at a high shear rate. *Blood, The Journal of the American Society of Hematology* **2015**, *125*, 881–888.
76. Zainal Abidin, N.A.; Timofeeva, M.; Szydzik, C.; Akbaridoust, F.; Lav, C.; Marusic, I.; Mitchell, A.; Hamilton, J.R.; Ooi, A.S.H.; Nesbitt, W.S. A microfluidic method to investigate platelet mechanotransduction under extensional strain. *Res Pract Thromb Haemost* **2023**, *7*, 100037.
77. Frojmovic, M.M.; Panjwani, R. Geometry of normal mammalian platelets by quantitative microscopic studies. *Biophysical journal* **1976**, *16*, 1071–1089.
78. Chesnutt, J.K.; Han, H.C. Platelet size and density affect shear-induced thrombus formation in tortuous arterioles. *Physical biology* **2013**, *10*, 056003.

 doi:10.20944/preprints202402.0799.v1

79. Litvinenko, A.; Moskalensky, A.; Karmadonova, N.; Nekrasov, V.; Strokotov, D.; Konokhova, A.; Yurkin, M.; Pokushalov, E.; Chernyshev, A.; Maltsev, V. Fluorescence-free flow cytometry for measurement of shape index distribution of resting, partially activated, and fully activated platelets. *Cytometry Pt A* **2016**, *89*, 1010–1016.
80. Hartwig, J.H. The platelet: form and function. In Proceedings of the Seminars in hematology. Elsevier, 2006, Vol. 43, pp. S94–S100.
81. White, J.G., CHAPTER 3 - Platelet Structure. In *Platelets (Second Edition)*; Michelson, A.D., Ed.; Academic Press: Burlington, 2007; pp. 45–73.
82. Raucher, D.; Sheetz, M.P. Characteristics of a membrane reservoir buffering membrane tension. *Biophysical journal* **1999**, *77*, 1992–2002.
83. Moskalensky, A.E.; Litvinenko, A.L. The platelet shape change: biophysical basis and physiological consequences. *Platelets* **2019**, *30*, 543–548.
84. White, J.G.; Rao, G. Microtubule coils versus the surface membrane cytoskeleton in maintenance and restoration of platelet discoid shape. *The American journal of pathology* **1998**, *152*, 597.
85. Italiano Jr, J.E.; Bergmeier, W.; Tiwari, S.; Falet, H.; Hartwig, J.H.; Hoffmeister, K.M.; André, P.; Wagner, D.D.; Shivdasani, R.A. Mechanisms and implications of platelet discoid shape. *Blood* **2003**, *101*, 4789–4796.
86. Hartwig, J.H.; DeSisto, M. The cytoskeleton of the resting human blood platelet: structure of the membrane skeleton and its attachment to actin filaments. *The Journal of cell biology* **1991**, *112*, 407–425.
87. Hartwig, J.; Barkalow, K.; Azim, A.; Italiano, J. The Elegant Platelet: Signals Controlling Actin Assembly. *Thromb Haemost* **1999**, *82*, 392–398.
88. Ajzenberg, N.; Haghighat Talab, A.T.; Massé, J.M.; Drouin, A.; Jondeau, K.; Kobeiter, H.; Baruch, D.; Cramer, E.M. Platelet shape change and subsequent glycoprotein redistribution in human stenosed arteries. *Platelets* **2005**, *16*, 13–18.
89. Du Plooy, J.N.; Buys, A.; Duim, W.; Pretorius, E. Comparison of platelet ultrastructure and elastic properties in thrombo-embolic ischemic stroke and smoking using atomic force and scanning electron microscopy. *PLoS One* **2013**, *8*, e69774.
90. Wurzinger, L.J.; Blasberg, P.; Schmid-Schönbein, H. Towards a concept of thrombosis in accelerated flow: rheology, fluid dynamics, and biochemistry. *Biorheology* **1985**, *22*, 437–450.
91. Wurzinger, L.J.; Opitz, R.; Wolf, M.; Schmid-Schnöbein, H. Ultrastructural investigations on the question of mechanical activation of blood platelets. *Blut* **1987**, *54*, 97–107.
92. Purvis Jr, N.B.; Giorgio, T.D. The effects of elongational stress exposure on the activation and aggregation of blood platelets. *Biorheology* **1991**, *28*, 355–367.
93. Chen, Z.; Mondal, N.K.; Ding, J.; Gao, J.; Griffith, B.P.; Wu, Z.J. Shear-induced platelet receptor shedding by non-physiological high shear stress with short exposure time: glycoprotein Ibα and glycoprotein VI. *Thrombosis research* **2015**, *135*, 692–698.
94. Chen, Z.; Mondal, N.K.; Ding, J.; Koenig, S.C.; Slaughter, M.S.; Griffith, B.P.; Wu, Z.J. Activation and shedding of platelet glycoprotein IIb/IIIa under non-physiological shear stress. *Mol Cell Biochem* **2015**, *409*, 93–101.
95. Chen, Z.; Mondal, N.K.; Zheng, S.; Koenig, S.C.; Slaughter, M.S.; Griffith, B.P.; Wu, Z.J. High shear induces platelet dysfunction leading to enhanced thrombotic propensity and diminished hemostatic capacity. *Platelets* **2019**, *30*, 112–119.
96. Holme, P.A.; Ørvim, U.; Hamers, M.J.A.G.; Solum, N.O.; Brosstad, F.R.; Barstad, R.M.; Sakariassen, K.S. Shear-Induced Platelet Activation and Platelet Microparticle Formation at Blood Flow Conditions as in Arteries With a Severe Stenosis. *ATVB* **1997**, *17*, 646–653.
97. Jones, C.I. Platelet function and ageing. *Mammalian Genome* **2016**, *27*, 358–366. Place: New York Publisher: Springer US.
98. Cowman, J.; Dunne, E.; Oglesby, I.; Byrne, B.; Ralph, A.; Voisin, B.; Müllers, S.; Ricco, A.J.; Kenny, D. Age-related changes in platelet function are more profound in women than in men. *Scientific reports* **2015**, *5*, 12235–12235. Place: England Publisher: Nature Publishing Group.
99. Kuhnla, A.; Reinthaler, M.; Braune, S.; Maier, A.; Pindur, G.; Lendlein, A.; Jung, F. Spontaneous and induced platelet aggregation in apparently healthy subjects in relation to age. *Clinical hemorheology and microcirculation* **2019**, *71*, 425–435.

 doi:10.20944/preprints202402.0799.v1

100. Sola-Visner, M. Platelets in the neonatal period: developmental differences in platelet production, function, and hemostasis and the potential impact of therapies. *Hematology 2010, the American Society of Hematology Education Program Book* **2012**, *2012*, 506–511.
101. Gelman, B.; Setty, B.N.; Chen, D.; Amin-Hanjani, S.; Stuart, M.J. Impaired mobilization of intracellular calcium in neonatal platelets. *Pediatric research* **1996**, *39*, 692–696.
102. Israels, S.J.; Rand, M.L.; Michelson, A.D. Neonatal platelet function. In Proceedings of the Seminars in thrombosis and hemostasis. Copyright© 2003 by Thieme Medical Publishers, Inc., 333 Seventh Avenue, New . . . , 2003, Vol. 29, pp. 363–372.
103. Sitaru, A.; Holzhauer, S.; Speer, C.; Singer, D.; Obergfell, A.; Walter, U.; Grossmann, R. Neonatal platelets from cord blood and peripheral blood. *Platelets* **2005**, *16*, 203–210.
104. Bernhard, H.; Rosenkranz, A.; Novak, M.; Leschnik, B.; Petritsch, M.; Rehak, T.; Köfeler, H.; Ulrich, D.; Muntean, W. No differences in support of thrombin generation by neonatal or adult platelets. *Hamostaseologie* **2009**, *29*, S94–S97.
105. Cvirn, G.; Gallistl, S.; Rehak, T.; Jürgens, G.; Muntean, W. Elevated thrombin-forming capacity of tissue factor-activated cord compared with adult plasma. *Journal of Thrombosis and Haemostasis* **2003**, *1*, 1785–1790.
106. Muntean, W.; Leschnik, B.; Baier, K.; Cvirn, G.; Gallistl, S. In vivo thrombin generation in neonates. *Journal of Thrombosis and Haemostasis* **2004**, *2*, 2071–2072.
107. Baker-Groberg, S.; Lattimore, S.; Recht, M.; McCarty, O.; Haley, K. Assessment of neonatal platelet adhesion, activation, and aggregation. *Journal of Thrombosis and Haemostasis* **2016**, *14*, 815–827.
108. Levy-Shraga, Y.; Maayan-Metzger, A.; Lubetsky, A.; Shenkman, B.; Kuint, J.; Martinowitz, U.; Kenet, G. Platelet function of newborns as tested by cone and plate (let) analyzer correlates with gestational age. *Acta haematologica* **2006**, *115*, 152–156.
109. Sheriff, J.; Malone, L.E.; Avila, C.; Zigomalas, A.; Bluestein, D.; Bahou, W.F. Shear-Induced Platelet Activation is Sensitive to Age and Calcium Availability: A Comparison of Adult and Umbilical Cord Blood. *Cell Mol Bioeng* **2020**, *13*, 575–590.
110. Caparros-Perez, E.; Teruel-Montoya, R.; López-Andreo, M.J.; Llanos, M.C.; Rivera, J.; Palma-Barqueros, V.; Blanco, J.E.; Vicente, V.; Martínez, C.; Ferrer-Marín, F. Comprehensive comparison of neonate and adult human platelet transcriptomes. *PLoS One* **2017**, *12*, e0183042.
111. Saving, K.L.; Jennings, D.E.; Aldag, J.C.; Caughey, R.C. Platelet ultrastructure of high-risk premature infants. *Thrombosis research* **1994**, *73*, 371–384.
112. Mody, N.A.; King, M.R. Three-dimensional simulations of a platelet-shaped spheroid near a wall in shear flow. *Physics of Fluids* **2005**, *17*.
113. Mody, N.A.; King, M.R. Platelet adhesive dynamics. Part I: characterization of platelet hydrodynamic collisions and wall effects. *Biophysical journal* **2008**, *95*, 2539–2555.
114. Mody, N.A.; King, M.R. Platelet adhesive dynamics. Part II: high shear-induced transient aggregation via GPIbα-vWF-GPIbα bridging. *Biophysical journal* **2008**, *95*, 2556–2574.
115. Pozrikidis, C. Flipping of an adherent blood platelet over a substrate. *Journal of Fluid Mechanics* **2006**, *568*, 161–172.
116. Sweet, C.R.; Chatterjee, S.; Xu, Z.; Bisordi, K.; Rosen, E.D.; Alber, M. Modelling platelet–blood flow interaction using the subcellular element Langevin method. *J. R. Soc. Interface.* **2011**, *8*, 1760–1771.
117. Wu, Z.; Xu, Z.; Kim, O.; Alber, M. Three-dimensional multi-scale model of deformable platelets adhesion to vessel wall in blood flow. *Phil. Trans. R. Soc. A.* **2014**, *372*, 20130380.
118. Zhang, P.; Gao, C.; Zhang, N.; Slepian, M.J.; Deng, Y.; Bluestein, D. Multiscale Particle-Based Modeling of Flowing Platelets in Blood Plasma Using Dissipative Particle Dynamics and Coarse Grained Molecular Dynamics. *Cel. Mol. Bioeng.* **2014**, *7*, 552–574.
119. Zhang, P.; Zhang, L.; Slepian, M.J.; Deng, Y.; Bluestein, D. A multiscale biomechanical model of platelets: Correlating with in-vitro results. *Journal of biomechanics* **2017**, *50*, 26–33.
120. Pothapragada, S.; Zhang, P.; Sheriff, J.; Livelli, M.; Slepian, M.J.; Deng, Y.; Bluestein, D. A phenomenological particle-based platelet model for simulating filopodia formation during early activation. *Numer Methods Biomed Eng* **2015**, *31*, e02702.
121. Zhang, P.; Sheriff, J.; Einav, S.; Slepian, M.J.; Deng, Y.; Bluestein, D. A predictive multiscale model for simulating flow-induced platelet activation: Correlating in silico results with in vitro results. *Journal of biomechanics* **2021**, *117*, 110275.

122. Maxwell, M.J.; Westein, E.; Nesbitt, W.S.; Giuliano, S.; Dopheide, S.M.; Jackson, S.P. Identification of a 2-stage platelet aggregation process mediating shear-dependent thrombus formation. *Blood* **2007**, *109*, 566–576.
123. Ruggeri, Z.M. Mechanisms Initiating Platelet Thrombus Formation. *Thromb Haemost* **1997**, *78*, 611–616.
124. Fogelson, A.L.; Neeves, K.B. Fluid Mechanics of Blood Clot Formation. *Annu. Rev. Fluid Mech.* **2015**, *47*, 377–403.
125. Flamm, M.H.; Colace, T.V.; Chatterjee, M.S.; Jing, H.; Zhou, S.; Jaeger, D.; Brass, L.F.; Sinno, T.; Diamond, S.L. Multiscale prediction of patient-specific platelet function under flow. *Blood, The Journal of the American Society of Hematology* **2012**, *120*, 190–198.
126. Gupta, P.; Zhang, P.; Sheriff, J.; Bluestein, D.; Deng, Y. A Multiscale Model for Recruitment Aggregation of Platelets by Correlating with In Vitro Results. *Cel. Mol. Bioeng.* **2019**, *12*, 327–343.
127. Gupta, P.; Zhang, P.; Sheriff, J.; Bluestein, D.; Deng, Y. A multiscale model for multiple platelet aggregation in shear flow. *Biomech Model Mechanobiol* **2021**, *20*, 1013–1030.
128. Fogelson, A.L.; Guy, R.D. Immersed-boundary-type models of intravascular platelet aggregation. *Computer methods in applied mechanics and engineering* **2008**, *197*, 2087–2104.
129. Mori, D.; Yano, K.; Tsubota, K.i.; Ishikawa, T.; Wada, S.; Yamaguchi, T. Simulation of platelet adhesion and aggregation regulated by fibrinogen and von Willebrand factor. *Thromb Haemost* **2008**, *99*, 108–115.
130. Shankar, K.N.; Zhang, Y.; Sinno, T.; Diamond, S.L. A three-dimensional multiscale model for the prediction of thrombus growth under flow with single-platelet resolution. *PLoS computational biology* **2022**, *18*, e1009850.
131. Du, J.; Kim, D.; Alhawael, G.; Ku, D.N.; Fogelson, A.L. Clot permeability, agonist transport, and platelet binding kinetics in arterial thrombosis. *Biophysical journal* **2020**, *119*, 2102–2115.
132. Du, J.; Fogelson, A.L. A computational investigation of occlusive arterial thrombosis. *Biomech Model Mechanobiol* **2023**.
133. Maxwell, M.J.; Westein, E.; Nesbitt, W.S.; Giuliano, S.; Dopheide, S.M.; Jackson, S.P. Identification of a 2-stage platelet aggregation process mediating shear-dependent thrombus formation. *Blood* **2007**, *109*, 566–576.
134. Chatterjee, M.S.; Purvis, J.E.; Brass, L.F.; Diamond, S.L. Pairwise agonist scanning predicts cellular signaling responses to combinatorial stimuli. *Nature biotechnology* **2010**, *28*, 727–732.
135. Zhou, Y.; Yasumoto, A.; Lei, C.; Huang, C.J.; Kobayashi, H.; Wu, Y.; Yan, S.; Sun, C.W.; Yatomi, Y.; Goda, K. Intelligent classification of platelet aggregates by agonist type. *Elife* **2020**, *9*, e52938.
136. Kempster, C.; Butler, G.; Kuznecova, E.; Taylor, K.A.; Kriek, N.; Little, G.; Sowa, M.A.; Sage, T.; Johnson, L.J.; Gibbins, J.M. Fully automated platelet differential interference contrast image analysis via deep learning. *Scientific reports* **2022**, *12*, 4614.
137. Zhang, Z.; Zhang, P.; Wang, P.; Sheriff, J.; Bluestein, D.; Deng, Y. Rapid analysis of streaming platelet images by semi-unsupervised learning. *Computerized Medical Imaging and Graphics* **2021**, *89*, 101895.
138. Sheriff, J.; Wang, P.; Zhang, P.; Zhang, Z.; Deng, Y.; Bluestein, D. In Vitro Measurements of Shear-Mediated Platelet Adhesion Kinematics as Analyzed through Machine Learning. *Ann Biomed Eng* **2021**, *49*, 3452–3464.
139. Zhang, Z.; Zhang, P.; Han, C.; Cong, G.; Yang, C.C.; Deng, Y. Online machine learning for accelerating molecular dynamics modeling of cells. *Frontiers in Molecular Biosciences* **2022**, *8*, 812248.
140. Zitnik, M.; Nguyen, F.; Wang, B.; Leskovec, J.; Goldenberg, A.; Hoffman, M.M. Machine learning for integrating data in biology and medicine: Principles, practice, and opportunities. *Information Fusion* **2019**, *50*, 71–91.
141. Shankar, K.N.; Zhang, Y.; Sinno, T.; Diamond, S.L. A three-dimensional multiscale model for the prediction of thrombus growth under flow with single-platelet resolution. *PLoS computational biology* **2022**, *18*, e1009850.
142. Han, C.; Zhang, P.; Zhu, Y.; Cong, G.; Kozloski, J.R.; Yang, C.C.; Zhang, L.; Deng, Y. Scalable multiscale modeling of platelets with 100 million particles. *J Supercomput* **2022**, *78*, 19707–19724.
143. Zhu, Y.; Han, C.; Zhang, P.; Cong, G.; Kozloski, J.R.; Yang, C.C.; Zhang, L.; Deng, Y. AI-aided multiscale modeling of physiologically-significant blood clots. *Computer Physics Communications* **2023**, *287*, 108718.